

# Kaon optical potential in nuclei and kaon condensation in neutron star

C. Y. Ryu,<sup>1,\*</sup> C. H. Hyun,<sup>2,†</sup> S. W. Hong,<sup>3,‡</sup> and B. T. Kim<sup>3,§</sup>

<sup>1</sup>*Department of Physics, Sungkyunkwan University, Suwon 440-746, Korea*

<sup>2</sup>*Department of Physics, Sungkyunkwan University, Suwon 440-746, Korea  
School of Physics, Seoul National University, Seoul 151-742, Korea*

<sup>3</sup>*Department of Physics, Sungkyunkwan University, Suwon 440-746, Korea*

## Abstract

Recent experiments at KEK, BNL, and DAΦNE revealed very interesting peaks that might be interpreted as deeply bound kaonic nuclear systems, which were predicted by Akaishi and Yamazaki. If those peaks are indeed deeply bound kaonic nuclear states, it implies that the real part of the kaon optical potential is very large. We consider this possibility and try to fix the coupling constants for strange quarks within the framework of a modified quark-meson coupling model. We then apply the modified quark-meson coupling model to the neutron star matter and obtain the equation of state and the maximum mass of a neutron star. It is found that the equation of state, composition of matter and properties of a neutron star are very sensitive to the interaction strength of a kaon in matter. We find interesting critical phenomena when the magnitude of the real part of the kaon optical potential in matter at the saturation density becomes as large as 140 MeV.

---

\*Electronic address: cyryu@color.skku.ac.kr

†Electronic address: hch@meson.skku.ac.kr

‡Electronic address: swhong@skku.ac.kr

§Electronic address: btkim@skku.ac.kr

## I. INTRODUCTION

The interior of a neutron star is believed to have great diversity. At nuclear matter densities around the saturation density  $\rho_0$ , the matter is composed of nucleons, electrons and muons, and it is mostly populated by the neutrons to satisfy the  $\beta$ -equilibrium, charge neutrality and Pauli blocking. At densities higher than  $\rho_0$ , maybe at  $\rho \geq 2\rho_0$ , the situation becomes quite unclear. Many possibilities have been proposed; creation of hyperons [1], pion [2] or kaon [3] condensation, strange matter [4], quark deconfinement [5, 6, 7] and etc. It is, at present, very difficult to predict what the interior of a neutron star looks like, but to some extent we may formulate the dynamics and draw some pictures by exploring various properties of a neutron star.

In this work, we consider the possibility of hyperon creation and kaon condensation in the neutron star matter. The masses and energies of the hyperons and kaons in medium are sensitive to their interactions with surrounding nucleons. In the meson-exchange picture, meson-hyperon and meson-kaon coupling constants determine the strength of these interactions. The meson-hyperon coupling constants may be determined from the binding energies of a hyperon in hypernuclei, for instance. The meson-kaon coupling constants have been studied by using the kaon-nucleon scattering and kaonic atom data. Some calculations [8, 9, 10] show that the real part of the  $K^-$ -nucleus optical potential  $U_{K^-}$  is shallow ( $U_{K^-} \approx -50$  MeV), but some other calculations [11, 12] suggest that  $U_{K^-}$  can be as large as about  $-120$  MeV or even close to  $-200$  MeV [13].

Recently, Akaishi and Yamazaki predicted the existence of deeply bound kaonic nuclei [14], in which  $U_{K^-}$  at normal density  $\rho_0$  is estimated to be about  $-120$  MeV. Observations of the tribaryon kaonic nuclei,  $S^0$  [15] and  $S^+$  [16] seem to indicate that  $K^-$  may be even more deeply bound in a nucleus than the theoretical prediction [14]. A BNL experiment with  $^{16}\text{O}(K^-, n)$  reaction [17] and FINUDA collaboration at DAΦNE [18] also reported distinct peaks. The identities of these peaks need to be studied further experimentally and theoretically. However, in this work, we consider the possibility of deep optical potential of kaons and apply such deep potentials to neutron star matter to study the consequences in the equation of state (EoS) of dense matter and neutron star properties.

We employ the modified quark-meson coupling (MQMC) model [19] for the description of dense matter. Nucleons and hyperons in the baryon octet are described as MIT bags.

The bag constant  $B_B$  and phenomenological constant  $Z_B$  for baryon  $B$  are determined to reproduce the free mass of each baryon. Coupling constants between  $(u, d)$ -quarks and  $(\sigma, \omega, \rho)$ -mesons are adjusted to produce the saturation density  $\rho_0 = 0.17 \text{ fm}^{-3}$ , binding energy per a nucleon  $E_b/A = 16 \text{ MeV}$  and symmetry energy at the saturation  $a_{\text{sym}} = 32.5 \text{ MeV}$ . Since the interaction between the  $s$ -quark and mesons are not well known, we adopt the standard quark counting rule and assume the  $s$ -quark is decoupled to  $(\sigma, \omega, \rho)$ -mesons. To take into account the interactions between  $s$ -quarks, we introduce  $\sigma^*(f_0(980))$  and  $\phi(1020)$  mesons following Ref. [20]. The coupling constants between the  $s$ -quark and  $(\sigma^*, \phi)$ -mesons are fixed by SU(6) symmetry. In this work we assume the kaon as a point particle. This treatment allows us to use  $U_{K^-}$  as an input to fix the kaon-meson coupling constants. In our model the real part of the optical potential can be written as  $U_{K^-} = -(g_{\sigma K}\sigma(\rho_0) + g_{\omega K}\omega(\rho_0))$ , where  $\sigma(\rho_0)$  and  $\omega(\rho_0)$  are the values of the meson fields at  $\rho_0$ . By using the value of  $g_{\omega K}$  given by the quark counting rule, we can determine  $g_{\sigma K}$  for each given value of  $U_{K^-}$ . Once the parameters of the model are fixed, the composition profile of neutron star matter can be obtained from  $\beta$ -equilibrium and charge neutrality. Then EoS can be easily obtained by computing the energy density and the pressure. The EoS is inserted in the Tolman-Oppenheimer-Volkoff equation to give a mass-radius relation of a stable neutron star. We find that the composition of neutron star matter changes dramatically depending on the value of  $U_{K^-}$  and that the maximum mass and radius of a neutron star also change sizably.

## II. THEORY

### A. Model

The model Lagrangian comprises the octet baryon, lepton and kaon terms:  $\mathcal{L}_{\text{tot}} = \mathcal{L}_B + \mathcal{L}_l + \mathcal{L}_K$ . Octet baryon and lepton terms in the mean field approximation can be written as

$$\begin{aligned} \mathcal{L}_B + \mathcal{L}_l = & \sum_B \bar{\psi}_B \left[ i\gamma \cdot \partial - m_B^*(\sigma, \sigma^*) - \gamma^0 \left( g_{\omega B}\omega_0 + g_{\phi B}\phi_0 + \frac{1}{2}g_{\rho B}\tau_z\rho_{03} \right) \right] \psi_B \\ & + \frac{1}{2} \left( -m_\sigma^2\sigma^2 - m_{\sigma^*}^2\sigma^{*2} + m_\omega^2\omega_0^2 + m_\phi^2\phi_0^2 + m_\rho^2\rho_{03}^2 \right) + \sum_l \bar{\psi}_l (i\gamma \cdot \partial - m_l)\psi_l, \end{aligned} \quad (1)$$

where  $B$  denotes the sum over all the baryon octet ( $p, n, \Lambda, \Sigma^+, \Sigma^0, \Sigma^-, \Xi^0, \Xi^-$ ), and  $l$  stands for the sum over the free electrons and muons ( $e^-, \mu^-$ ).  $\sigma, \omega$  and  $\rho$  mesons account for the interactions between the non-strange light quarks ( $u$  and  $d$ ).  $\sigma^*$  and  $\phi$  mesons mediate

interactions between  $s$  quarks.

In the MQMC model, the effective mass of a baryon  $m_B(\sigma, \sigma^*)$  can be written as [20, 21]

$$m_B^* = \sqrt{E_B^2 - \sum_q \left(\frac{x_q}{R}\right)^2}. \quad (2)$$

The bag energy of a baryon is given by

$$E_B = \sum_q \frac{\Omega_q}{R} - \frac{Z_B}{R} + \frac{4}{3}\pi R^3 B_B, \quad (3)$$

where  $B_B$  and  $Z_B$  are the bag constant and a phenomenological constant for the zero-point motion of a baryon  $B$ , respectively.  $\Omega_q = \sqrt{x_q^2 + (Rm_q^*)^2}$ , where  $m_q^*(= m_q - g_\sigma^q \sigma - g_{\sigma^*}^q \sigma^*)$  is the effective mass of a quark whose free mass is  $m_q$ . We take  $m_q = 0$  for  $q = u, d$  and  $m_q = 150$  MeV for  $q = s$ .  $x_q$  is determined from the boundary condition on the bag surface  $r = R$ ,

$$j_0(x_q) = \beta_q j_1(x_q), \quad (4)$$

where  $\beta_q = \sqrt{\frac{\Omega_q - Rm_q^*}{\Omega_q + Rm_q^*}}$ . In the MQMC model, the bag constant  $B_B$  is assumed to depend on density. In this work, we extend the form used in [19] to include the contribution from  $\sigma^*$  as

$$B_B(\sigma, \sigma^*) = B_{B0} \exp \left\{ -4g_\sigma'^B \left( \sum_{q=u,d} n_q \sigma + (3 - \sum_{q=u,d} n_q) \sqrt{2} \sigma^* \right) / m_B \right\}, \quad (5)$$

where  $m_B$  is the bare mass of the baryon  $B$ . Note that the exponent on the right hand side of Eq. (5) shows that  $\sigma$  meson couples only to  $u$  and  $d$  quarks, and  $\sigma^*$  meson only to  $s$  quark. The factor  $\sqrt{2}$  in front of  $\sigma^*$  is introduced due to SU(6) symmetry.

The effective Lagrangian for the kaon can be expressed as [22]

$$\mathcal{L}_K = D_\mu^* K^* D^\mu K - m_K^{*2} K^* K, \quad (6)$$

where  $D_\mu = \partial_\mu + ig_{\omega K} \omega_\mu - ig_{\phi K} \phi_\mu + i\frac{1}{2}g_{\rho K} \vec{\tau} \cdot \vec{\rho}_\mu$ , and the effective mass of a kaon as a point particle is given by

$$m_K^* = m_K - g_{\sigma K} \sigma - g_{\sigma^* K} \sigma^*. \quad (7)$$

The equation of motion for a kaon is obtained as

$$[D_\mu D^\mu + m_K^{*2}]K(x) = 0. \quad (8)$$

$g_\sigma^q$	$g_\omega^q$	$g_\sigma^{\prime B}$	$g_\rho^q$	$m_N^*/m_N$	$K$ (MeV)
1.0	2.71	2.27	7.89	0.78	285.5

TABLE I: The coupling constants for ( $u$ ,  $d$ )-quarks and ( $\sigma$ ,  $\omega$ ,  $\rho$ )-mesons in the MQMC model to reproduce the binding energy  $E_b/A = 16$  MeV at the saturation density  $0.17 \text{ fm}^{-3}$  and symmetry energy  $a_{\text{sym}} = 32.5$  MeV.  $m_N^*/m_N$  and  $K$  are the effective mass ratio to the free mass of the nucleon and the compression modulus at the saturation density, respectively.

In uniform infinite matter, the kaon field  $K(x)$  can be written as a plane wave. Substituting the plane wave solution into the equation of motion, we obtain the dispersion relation for the anti-kaon

$$\omega_K = m_K^* - g_{\omega K}\omega_0 + g_{\phi K}\phi_0 - g_{\rho K}I_{3K}\rho_0, \quad (9)$$

where  $I_{3K}$  is the isospin third component of the anti-kaon. (In this work it is the anti-kaon  $K^-$  that plays an important role, but we shall refer to both kaons and anti-kaons just as kaons for brevity.)

## B. Model parameters

MIT bag parameters  $B_B$  and  $Z_B$  are determined to reproduce the free mass of a baryon  $B$ ,  $m_B^*|_{\rho=0} = m_B$ , at a given bag radius, which we choose as  $R_0 = 0.6$  fm, with the minimization condition  $\left. \frac{\partial m_B}{\partial R} \right|_{R=R_0} = 0$ .

Three conditions  $\rho_0$ ,  $E_b/A$ , and  $a_{\text{sym}}$  could determine three quark-meson coupling constants  $g_\sigma^{u,d}$ ,  $g_\omega^{u,d}$  and  $g_\rho^{u,d}$ , assuming  $u$  and  $d$  quarks are identical particles in an isodoublet. But as seen in Eq. (5), use of the MQMC model introduces an additional constant  $g_\sigma^{\prime B}$ , and thus four coupling constants cannot be determined uniquely. Thus we fix  $g_\sigma^q = 1$ , and adjust the remaining three constants to satisfy the three conditions. The obtained coupling constants are given in Table I, where the resulting mass ratio of the nucleon,  $m_N^*/m_N$ , and the compression modulus  $K$  at the saturation density are also given. The MQMC model produces  $m_N^*$  and  $K$  within reasonable ranges;  $m_N^* = (0.7 \sim 0.8)m_N$  and  $K = (200 \sim 300)$  MeV. The coupling constants between  $s$ -quarks and mesons cannot be determined from the conditions at the saturation density. In principle, experimental data from hypernuclei,

$ U_{K^-} $ (MeV)	80	100	120	140	160
$g_{\sigma K}$	1.25	2.01	2.75	3.50	4.25

TABLE II:  $g_{\sigma K}$  determined for several  $U_{K^-}$  values.

kaon-nucleus scattering and kaonic atom could be used to determine meson-hyperon coupling constants. However, at present these coupling constants are not well known, and for simplicity we assume that the  $s$  quark does not interact with  $u$  and  $d$  quarks. Then we have

$$g_{\sigma}^s = g_{\omega}^s = g_{\rho}^s = 0. \quad (10)$$

For the meson-baryon coupling constants, we use the quark counting rule, which gives us the relations

$$\begin{aligned} g_{\omega}^q &= \frac{1}{3}g_{\omega N} = \frac{1}{2}g_{\omega\Lambda} = \frac{1}{2}g_{\omega\Sigma} = g_{\omega\Xi}, \\ g_{\rho}^q &= g_{\rho N} = g_{\rho\Sigma} = g_{\rho\Xi}, \quad g_{\rho\Lambda} = 0, \\ g_{\phi}^s &= g_{\phi\Lambda} = g_{\phi\Sigma} = \frac{1}{2}g_{\phi\Xi}, \end{aligned} \quad (11)$$

where  $g_{\phi}^s = \sqrt{2}g_{\omega}^{u,d}$  from the SU(6) symmetry. With the quark-meson coupling constants given in Table I and Eq. (10), the meson-baryon couplings are completely determined through Eq. (11).

For the meson-kaon coupling constants,  $g_{\omega K}$  and  $g_{\rho K}$  may be fixed by the quark counting rule;  $g_{\omega K} = g_{\omega}^q$  and  $g_{\rho K} = g_{\rho}^q$ . Also,  $g_{\sigma^* K}$  and  $g_{\phi K}$  can be determined from SU(6) symmetry;  $g_{\sigma^* K} = \sqrt{2}g_{\sigma K}$  and  $g_{\phi K} = \sqrt{2}g_{\omega K}$ . Then the remaining coupling constant,  $g_{\sigma K}$ , can be related to the real part of the optical potential of a kaon at the saturation density;  $U_{K^-} = -(g_{\sigma K}\sigma + g_{\omega K}\omega_0)$ .  $g_{\sigma K}$  values thus determined are summarized for several  $U_{K^-}$  values in Table II.

### C. EoS of neutron star matter

To obtain the EoS, we need to determine the following 16 variables at each density: 5 meson fields ( $\sigma, \omega, \rho, \sigma^*, \phi$ ), 8 octet baryon densities, 2 lepton densities and the kaon density  $\rho_K$ . 5 meson fields can be determined from their equations of motion:

$$m_{\sigma}^2\sigma = \sum_B g_{\sigma B}C_B(\sigma) \frac{2J_B + 1}{2\pi^2} \int_0^{k_B} \frac{m_B^*}{[k^2 + m_B^{*2}]^{1/2}} k^2 dk + g_{\sigma K}\rho_K, \quad (12)$$

$$m_{\sigma^*}^2 \sigma^* = \sum_B g_{\sigma^* B} C_B(\sigma^*) \frac{2J_B + 1}{2\pi^2} \int_0^{k_B} \frac{m_B^*}{[k^2 + m_B^{*2}]^{1/2}} k^2 dk + g_{\sigma^* K} \rho_K, \quad (13)$$

$$m_\omega^2 \omega_0 = \sum_B g_{\omega B} (2J_B + 1) k_B^3 / (6\pi^2) - g_{\omega K} \rho_K, \quad (14)$$

$$m_\phi^2 \phi_0 = \sum_B g_{\phi B} (2J_B + 1) k_B^3 / (6\pi^2) + g_{\phi K} \rho_K, \quad (15)$$

$$m_\rho^2 \rho_{03} = \sum_B g_{\rho B} I_{3B} (2J_B + 1) k_B^3 / (6\pi^2) - g_{\rho K} I_{3K} \rho_K, \quad (16)$$

where  $J_B$  and  $I_{3B}$  are the spin and the isospin projection, respectively, and  $k_B$  is the Fermi momentum of the baryon species  $B$ . In Eqs. (12) and (13), the factors  $C_B(\sigma)$  and  $C_B(\sigma^*)$  are obtained by the conditions  $g_{\sigma B} C_B(\sigma) = -\frac{\partial m_B^*}{\partial \sigma}$  and  $g_{\sigma^* B} C_B(\sigma^*) = -\frac{\partial m_B^*}{\partial \sigma^*}$ .  $\beta$ -equilibrium of the baryons gives us 7 relations

$$\begin{aligned} \mu_n &= \mu_\Lambda = \mu_{\Sigma^0} = \mu_{\Xi^0}, \\ \mu_n + \mu_e &= \mu_{\Sigma^-} = \mu_{\Xi^-}, \\ \mu_n - \mu_e &= \mu_p = \mu_{\Sigma^+}, \end{aligned} \quad (17)$$

where the chemical potential of a baryon  $B$  is given by  $\mu_B = \sqrt{k_B^2 + m_B^{*2}(\sigma, \sigma^*)} + g_{\omega B} \omega_0 + g_{\phi B} \phi_0 + g_{\rho B} I_{3B} \rho_{03}$ . We assume leptons do not interact, and thus the chemical potential of a lepton  $l$  is simply written as  $\mu_l = \sqrt{k_l^2 + m_l^2}$ . The leptonic equilibration

$$\mu_e = \mu_\mu \quad (18)$$

determines the density of muons. As density increases, Fermi momentum of the electron increases, and at a density where the condition

$$\omega_K = \mu_e \quad (19)$$

is met, kaons become condensed. Finally, charge neutrality is expressed as

$$\sum_B q_B \rho_B - \rho_K - \rho_e - \rho_\mu = 0, \quad (20)$$

where  $q_B$  is the charge of baryon species  $B$  and  $\rho_B$  is the number density of  $B$ . Solving the Eqs. (12–20) self-consistently and simultaneously together with the quark eigenvalue

equation Eq. (4), one can determine the 16 variables uniquely. Once these 16 quantities are fixed, it is straightforward to compute the EoS by using the energy density

$$\begin{aligned} \varepsilon = & \frac{1}{2}m_\sigma^2\sigma^2 + \frac{1}{2}m_{\sigma^*}^2\sigma^{*2} + \frac{1}{2}m_\omega^2\omega_0^2 + \frac{1}{2}m_\phi^2\phi_0^2 + \frac{1}{2}m_\rho^2\rho_{03}^2 \\ & + \sum_B \frac{2J_B + 1}{2\pi^2} \int_0^{k_B} [k^2 + m_B^{*2}]^{1/2} k^2 dk + \sum_l \frac{1}{\pi^2} \int_0^{k_l} [k^2 + m_l^2]^{1/2} k^2 dk \\ & + m_K^* \rho_K, \end{aligned} \quad (21)$$

and the pressure

$$\begin{aligned} P = & -\frac{1}{2}m_\sigma^2\sigma^2 - \frac{1}{2}m_{\sigma^*}^2\sigma^{*2} + \frac{1}{2}m_\omega^2\omega_0^2 + \frac{1}{2}m_\phi^2\phi_0^2 + \frac{1}{2}m_\rho^2\rho_{03}^2 \\ & + \frac{1}{3} \sum_B \frac{2J_B + 1}{2\pi^2} \int_0^{k_B} \frac{k^4 dk}{[k^2 + m_B^{*2}]^{1/2}} + \frac{1}{3} \sum_l \frac{1}{\pi^2} \int_0^{k_l} \frac{k^4 dk}{[k^2 + m_l^2]^{1/2}}. \end{aligned} \quad (22)$$

Note that there is no contribution to the pressure coming from kaons because kaon momentum is set to zero.

### III. RESULTS

#### A. Composition of neutron star matter

Fig. 1 shows the composition profile of the neutron star matter for various  $U_{K^-}$  values. For a larger  $|U_{K^-}|$  value, kaons appear at lower densities. This behavior can be easily understood by noting that with a larger  $|U_{K^-}|$ ,  $g_{\sigma K}$  becomes larger, and as a result  $m_K^*$  becomes smaller. With a smaller  $m_K^*$ , the chemical equilibrium condition Eq. (19) that determines kaon condensation is fulfilled at a lower density, and this leads to an earlier onset of kaon condensation. For  $|U_{K^-}| = 80$  MeV, the kaon starts to appear at  $\rho \sim 4\rho_0$ . Since  $g_{\sigma K}(= 1.25)$  is relatively small, the effective mass of the kaon decreases slowly, and the creation of kaons is suppressed by the hyperons at higher densities. The population of the hyperons is slightly affected by the presence of the kaon, but the overall composition profile is in general the same as that without kaons. However, for  $|U_{K^-}| \geq 100$  MeV, the population of the hyperons, especially the number of negatively charged particles, is strongly affected by the presence of kaons. With a larger  $|U_{K^-}|$ , the effective mass of the kaon drops rapidly, and thus the kaon is favored more than the hyperons as a negatively charged particle with strangeness. Note that the densities where  $\Sigma^-$  and  $\Lambda$  are created

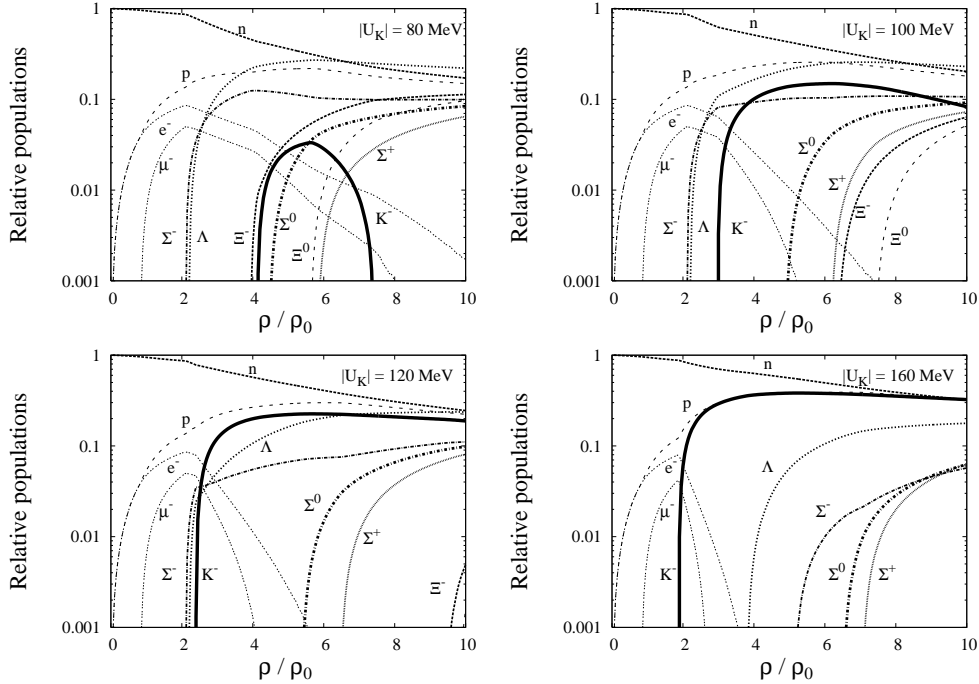


FIG. 1: Compositions of neutron star matter with octet baryons, electrons, muons and kaons.

remain the same for different values of  $U_{K^-}$  as long as the onset of the kaon condensation occurs later than the hyperon creation. However, as  $|U_{K^-}|$  gets larger than a critical value around 140 MeV, at which the kaon condensation appears prior to hyperon creation, the composition becomes dramatically different from the one without kaons. For instance, as shown in Fig. 1 for  $|U_{K^-}| = 160$  MeV the negative charges are predominately carried by the kaons, which suppresses the creation and population of the hyperons. When hyperon population becomes low, most of the positive charges are carried by the protons.

Let us compare our results with those in the literature. The properties of the kaon in nuclear matter [23] and the neutron star with kaon condensation [24] are investigated with the QMC (not the MQMC model we are using). In these calculations, a kaon is treated as an MIT bag, and the kaon- $\sigma$ ,  $-\omega$  and  $-\rho$  meson coupling constants are determined by the quark counting. In Ref. [23], it is discussed that the repulsion due to non-zero  $\rho$  meson field in the asymmetric matter makes kaon condensation less likely to occur. In Ref. [24], kaon condensation with hyperons is explicitly taken into account in the neutron star matter and is shown to occur at around  $4\rho_0$ . In Ref. [25], we have shown that the kaon-meson coupling constant from the quark counting rule gives us the same effective mass of the kaon as what

$ U_{K^-} $ (MeV)	80	100	120	140	160
$\rho_c/\rho_0$ (MQMC)	4.1	3.0	2.4	2.1	1.9
$\rho_c/\rho_0$ (without $\sigma^*$ and $\phi$ )	3.8	3.0	2.4	2.1	1.9

TABLE III: Onset densities of the kaon condensation  $\rho_c$  in the MQMC models for various  $U_{K^-}$  values. The third row shows the onset densities without including the  $\sigma^*$  and  $\phi$  mesons in the calculation.

we can get by using  $U_{K^-} = -100$  MeV. Our result for  $U_{K^-} = -100$  MeV from the MQMC model and Fig. 5 of [24] from the QMC model can be directly compared with each other. Ref. [24] shows kaons condense at densities higher than the densities where hyperons are created, but soon after the creation of kaons, the number of  $\Sigma^-$  quickly decreases and the population of kaons exceed that of hyperons. On the contrary, our results with  $U_{K^-} = -100$  MeV shows co-existence of the octet baryons together with kaons even at  $\rho \sim 10\rho_0$ .

To explore the effect of  $\sigma^*$  and  $\phi$ , we have calculated the onset density  $\rho_c$  of kaon condensation without  $\sigma^*$  and  $\phi$ , and the results are given in the third row of Table III. One can see that whether or not we include  $\sigma^*$  and  $\phi$  mesons does not make a significant difference in the condensation onset density. Since hyperons are the sources of these meson fields (see Eqs. (13) and (15)), at the densities where the population of the hyperons is not large the magnitudes of  $\sigma^*$  and  $\phi$  fields are quite small compared to those of  $\sigma$  and  $\omega$  mesons. Moreover, even when the magnitudes of  $\sigma^*$  and  $\phi$  become relatively large at higher densities, the contribution from  $\sigma^*$  to the energy of the kaon  $\omega_K$  has a sign opposite to that from  $\phi$ . Therefore, the effects of  $\sigma^*$  and  $\phi$  to the onset of the kaon condensation cancel out and become insignificant. It is worthwhile to note that if the kaons appear prior to the hyperons,  $\sigma^*$  and  $\phi$  mesons play no role to  $\rho_c$  since  $\sigma^*$ - and  $\phi$ -fields become non-zero only after the kaon density  $\rho_K$  becomes finite.

We have also investigated the effect of the coupling constants  $g_{\sigma^*K}$  and  $g_{\phi K}$ . The results shown in Table III are obtained by use of the constants determined by SU(6) symmetry, but  $g_{\sigma^*K}$  can also be fixed from  $f_0(980)$  decay [26], and  $g_{\phi K}$  can be determined from the SU(6) relation together with the value of  $g_{\pi\rho}$  as given by  $\sqrt{2}g_{\phi K} = g_{\pi\rho}$ .  $g_{\sigma^*K}$  and  $g_{\phi K}$  thus fixed are 2.65 and 4.27, respectively. We have used these new  $\sigma^*$ - and  $\phi$ - $K$  coupling constants to calculate the onset density of the kaon. The ratios  $\rho_c/\rho_0$  turn out to be 3.9, 3.0, 2.4, 2.1

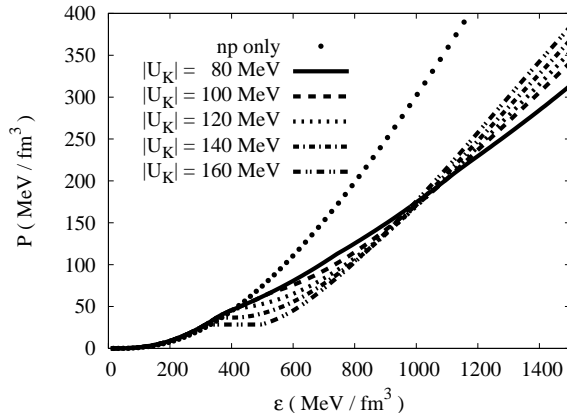


FIG. 2: The EoS of neutron star matter with only neutrons and protons (dots) and with including hyperons and kaon condensation for various  $U_{K^-}$  values.

and 1.9 for  $|U_{K^-}| = 80, 100, 120, 140$  and  $160$  MeV, respectively. Though different values of  $g_{\sigma^*K}$  and  $g_{\phi K}$  are used, the newly obtained ratios  $\rho_c/\rho_0$  are quite similar to the results presented in Table 3. It is again partly because the  $\sigma^*$ - and  $\phi$ -field values are small and partly because  $\sigma^*$  and  $\phi$  terms cancel each other in the energy of the kaon.

## B. EoS and neutron star bulk properties

The EoS for neutron star matter with octet baryons and kaons are plotted in Fig. 2 for various values of  $U_{K^-}$ . The EoS obtained by including only neutrons and protons (plotted by the dots) is above all the other EoS curves with including hyperons and kaons. When hyperons are included in the calculation, the EoS gets softened and becomes essentially the same as the EoS for  $U_{K^-} = -80$  MeV, so is not plotted in the figure. This also indicates that when  $U_{K^-} = -80$  MeV the composition of the matter is seldom affected by the kaon condensation. When  $|U_{K^-}|$  becomes larger, the formation of the kaon condensation softens further the EoS. When the kaon condensation takes place, one should take into account the phase transition from baryonic matter to mixed phase. Neutron star matter has two conserved charges; baryon number and electric charge. It was discussed in Ref. [22] that the Gibbs conditions have to be implemented for the description of the mixed phase in neutron star matter. For the sake of simplicity, however, we employ the Maxwell construction for the mixed phase in this work. Though not fully consistent, Maxwell construction can provide

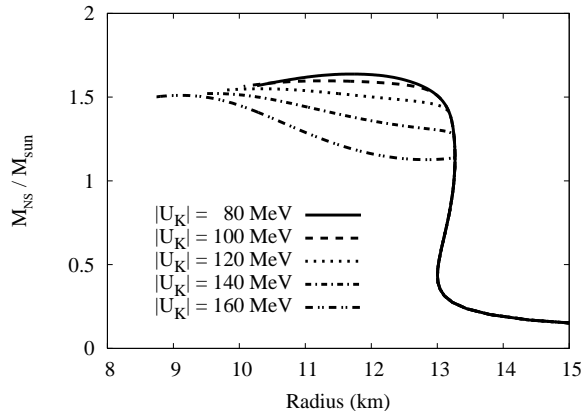


FIG. 3: Mass-radius relation of the neutron star with octet baryons and kaons. Mass is in units of the solar mass.

$ U_{K^-} $ (MeV)	80	100	120	140	160
$M_{\max}/M_{\odot}$	1.64	1.60	1.55	1.52	1.51
$R_{\max}$ (km)	11.7	11.3	10.3	9.6	9.1
$\rho_{\text{cen}}/\rho_0$	5.8	6.5	8.3	9.6	10.3

TABLE IV: Maximum mass in units of the solar mass and the corresponding radius and central density  $\rho_{\text{cen}}$  of a neutron star. Smaller maximum mass favors kaons than hyperons as strange particles.

reasonable results. Flat portions of the curves in Fig. 2 for  $|U_{K^-}| = 140$  and 160 MeV correspond to the mixed states with a constant pressure.

Bulk properties of the neutron star are obtained by solving the Tolman-Oppenheimer-Volkoff equation with the above EoS. Resulting mass-radius relations of the neutron star are shown in Fig. 3. The maximum mass, corresponding radius, and the central density of a stable neutron star for each EoS are given in Table IV. The mass-radius curve without kaons is almost the same as the curve for  $U_{K^-} = -80$  MeV as expected from the similarity of the EoS in the two cases and is not shown in the figure. As  $|U_{K^-}|$  increases, the maximum mass decreases monotonically. When  $|U_{K^-}|$  is larger than 120 MeV, the maximum mass changes slowly with  $|U_{K^-}|$ , but the two extreme cases  $|U_{K^-}| = 80$  and 160 MeV show a sizable difference ( $\sim 8\%$ ).

Let us compare our results with those in the literature. The maximum mass of a neutron star obtained from the QMC model [24] differs very much from what we have with the MQMC model. The QMC model without including kaons has the maximum mass  $1.98M_{\odot}$  which is about 20 % larger than the maximum mass  $1.64M_{\odot}$  from our MQMC model for  $U_{K^-} = -80$  MeV. (Note that the EoS for  $U_{K^-} = -80$  MeV is almost the same as that without kaons.) When kaons are included, our results from either  $U_{K^-} = -100$  or  $-120$  MeV can be compared to those of the QMC model [24] because these  $U_{K^-}$  values are in the range of  $U_{K^-}$  obtained by the QMC model (see Table 1 of Ref. [24]). When  $-120 \leq U_{K^-} \leq -100$  MeV, the MQMC model gives us the maximum mass of  $(1.55 \sim 1.60)M_{\odot}$ , but the QMC model produces  $1.94M_{\odot}$  for  $U_{K^-} = -123$  MeV. The role of the kaon condensation is, however, similar in both models. Kaon condensation makes the maximum mass smaller than without it. We can also compare the result of the MQMC model at  $U_{K^-} = -160$  MeV to that obtained from the quantum hadrodynamics (QHD) model with the same value of  $U_{K^-}$  [27]. The maximum mass from the QHD calculation is  $1.65M_{\odot}$  with the radius 10.8 km, while the MQMC model gives us  $1.51M_{\odot}$  with the radius 9.1 km. It should be noted, however, that in Ref. [27] the parameters are fitted to saturation conditions somewhat different from what we employ, and the Gibbs conditions are used for the description of the mixed phase. In Ref. [28], a thorough investigation was made of the dependence of the EoS on the conditions at the saturation density and the hyperon-meson coupling constants. It was shown that the result was sensitive to the choice of the saturation properties. Therefore, comparisons of the results from different models require careful attention to the input parameters and assumptions of the models.

#### IV. CONCLUSION

Using the modified quark-meson coupling model, we have obtained the composition profile of neutron star matter, the maximum mass and the radius of the neutron star, focusing on the role of the strange particles such as hyperons and kaons. Motivated by recent theoretical predictions of deeply bound kaonic states [14] and the subsequent observations of interesting peaks found in KEK, BNL and DAΦNE experiments, special attention is paid to the effect of large kaon optical potential  $U_{K^-}$  on the neutron star matter. By varying the value of  $U_{K^-}$ , we have investigated how the onset density of the kaon condensation, the composition

of the stellar matter, and the bulk properties of the neutron star change.

The onset density of the kaon condensation and the matter composition are found to be sensitive to the value of  $U_{K^-}$ . For  $|U_{K^-}| = 80$  MeV, kaons are produced at  $\rho \sim 4\rho_0$ , but their population does not build up due to the creation of hyperons. With  $|U_{K^-}| = 100$  MeV, the onset density is lowered down to  $3\rho_0$ , and at the densities around  $4 \leq \rho/\rho_0 \leq 8$ ,  $K^-$  is the most dominant negatively charged particle in matter. However, strangeness is still mostly carried by  $\Lambda$  hyperons. With  $|U_{K^-}| = 120$  MeV, kaons appear at densities close to those where the hyperons are created. Negative charges are dominantly carried by kaons, and strangeness is shared by kaons and  $\Lambda$ . For  $|U_{K^-}|$  larger than 120 MeV, kaon condensation takes place at around  $2\rho_0$ , and both negative charges and strangeness are dominantly carried by  $K^-$ . The model dependence of the onset density and the composition is discussed by comparing our results with other results in the literature. The MQMC model produces different results from the QMC model in both the onset density and the population of particles. The kaon condensation onset density depends little on the coupling constants  $g_{\sigma^*K}$  and  $g_{\phi K}$ .

Inclusion of hyperons and kaons makes the EoS softer than that with only nucleons. It shows that the strange particles play the role of making the neutron star more compact with smaller mass and smaller radius. Changes in  $U_{K^-}$  produce sizable effects on the maximum mass of the neutron star. With  $|U_{K^-}| = 160$  MeV, the maximum mass is  $1.51M_\odot$  in the MQMC model, which is about 8% smaller than that without kaon condensation. However, dependence of the kaon condensation on the parameters related to saturation properties and meson-baryon coupling constants requires further studies. The effect of these input parameters together with  $U_{K^-}$  values will be explored in future works.

## Acknowledgments

This work was supported by the Basic Research Program of the Korea Science & Engineering Foundation (R01-2005-000-10050-0) and by APCTP 2005 Topical Program. The authors thank Prof. Y. Akaishi for useful discussions.

---

[1] S. I. A. Garpman, N. K. Glendenning and Y. J. Karant, Nucl. Phys. **A322**, 382 (1979).

- [2] A. B. Migdal, *Rev. Mod. Phys.* **50**, 107 (1978).
- [3] D. B. Kaplan and A. E. Nelson, *Phys. Lett.* **B175**, 57 (1986).
- [4] A. R. Bodmer, *Phys. Rev. D* **4**, 1601 (1971).
- [5] N. Itoh, *Prog. Theor. Phys.* **44**, 291 (1970).
- [6] G. Baym and S. A. Chin, *Phys. Lett.* **B62**, 241 (1976).
- [7] B. D. Keister and K. S. Kisslinger, *Phys. Lett.* **B64**, 117 (1976).
- [8] J. Schaffner-Bielich, V. Koch and M. Effenberger, *Nucl. Phys.* **A669** 153 (2000).
- [9] A. Ramos and E. Oset, *Nucl. Phys.* **A671**, 481 (2000).
- [10] A. Cieply, E. Friedman, A. Gal and J. Mares, *Nucl. Phys.* **A696** 173 (2001).
- [11] E. Friedman, A. Gal and C. J. Batty, *Nucl. Phys.* **A579**, 578 (1994).
- [12] N. Kaiser, P.B. Siegel and W. Weise, *Nucl. Phys.* **A594** 325 (1995).
- [13] C. J. Batty, E. Friedman, A. Gal, *Phys. Rep.* **287**, 385 (1997).
- [14] T. Yamazaki and Y. Akaishi, *Phys. Lett.* **B535** 70 (2002); Y. Akaishi and T. Yamazaki, *Phys. Rev. C* **65**, 044005 (2002).
- [15] T. Suzuki *et al.*, *Phys. Lett.* **B597**, 263 (2004).
- [16] T. Suzuki *et al.*, *Nucl. Phys.* **A754**, 375c (2005).
- [17] T. Kishimoto *et al.*, *Nucl. Phys.* **A754**, 383 (2005).
- [18] M. Agnello *et al.*, *Phys. Rev. Lett.* **94**, 212303 (2005).
- [19] X. Jin and B. K. Jennings, *Phys. Lett.* **B374**, 13 (1996); *Phys. Rev. C* **54**, 1427 (1996).
- [20] S. Pal, M. Hanauske, I. Zakout, H. Stöcker and W. Greiner, *Phys. Rev. C* **60**, 015802 (1999).
- [21] S. Fleck, W. Bentz, K. Shimizu and K. Yazaki, *Nucl. Phys.* **A510**, 731 (1990).
- [22] N. K. Glendenning and J. Schaffner, *Phys. Rev. C* **60**, 025803 (1999).
- [23] K. Tsushima, K. Saito, A. W. Thomas and S. V. Wright, *Phys. Lett.* **B429**, 239 (1998).
- [24] D. P. Menezes, P. K. Panda and C. Providencia, *Phys. Rev. C* **72**, 035802 (2005).
- [25] C. Y. Ryu, C. H. Hyun, J. Y. Lee and S. W. Hong, *Phys. Rev. C* **72**, 045206 (2005).
- [26] T. A. Armstrong *et al.*, WA76 Collaboration, *Z. Phys. A* **51**, 351 (1991).
- [27] S. Banik and D. Bandyopadhyay, *Phys. Rev. C* **64**, 055805 (2001).
- [28] J. Schaffner and I. N. Mishustin, *Phys. Rev. C* **53**, 1416 (1996).

